Development of an Organic Rankine Cycle system for exhaust energy recovery in internal combustion engines

2015 J. Phys.: Conf. Ser. 655 012015

(http://iopscience.iop.org/1742-6596/655/1/012015)

Journal of Physics: Conference Series **655** (2015) 012015 doi:10.1088/1742-6596/655/1/012015

Development of an Organic Rankine Cycle system for exhaust energy recovery in internal combustion engines

Roberto Cipollone, Giuseppe Bianchi, Angelo Gualtieri, Davide Di Battista, Marco Mauriello, Fabio Fatigati

University of L′Aquila, via Giovanni Gronchi 18, L′Aquila 67100, Italy

E-mail: roberto.cipollone@univaq.it

Abstract. Road transportation is currently one of the most influencing sectors for global energy consumptions and CO_2 emissions. Nevertheless, more than one third of the fuel energy supplied to internal combustion engines is still rejected to the environment as thermal waste at the exhaust. Therefore, a greater fuel economy might be achieved recovering the energy from exhaust gases and converting it into useful power on board. In the current research activity, an ORC-based energy recovery system was developed and coupled with a diesel engine. The innovative feature of the recovery power unit relies upon the usage of sliding vane rotary machines as pump and expander. After a preliminary exhaust gas mapping, which allowed to assess the magnitude of the thermal power to be recovered, a thermodynamic analysis was carried out to design the ORC system and the sliding vane machines using R236fa as working fluid. An experimental campaign was eventually performed at different operating regimes according to the ESC procedure and investigated the recovery potential of the power unit at design and off-design conditions. Mechanical power recovered ranged from 0.7 kW up to 1.9 kW, with an overall cycle efficiency from 3.8% up to 4.8% respectively. These results candidate sliding vane machines as efficient and reliable devices for waste heat recovery applications.

1. Introduction

The current worldwide trend of increasing energy demand in road transportation sector remarkably contributes to the growing share of fossil fuel usage and to the release of harmful greenhouse gas emissions. To date, road transportation sector is currently responsible for 17% of the total share of global CO_2 emissions [1]. Nevertheless, the multitude of irreversible processes occurring in Internal Combustion Engines (ICEs) limit their capability to achieve a high efficiency. Indeed, a large amount of fuel energy is rejected from the engine to the environment as waste heat, with a significant fraction (30 - 40%) through the exhaust gases, whose outlet temperature makes them thermodynamically attractive. Hence, a conversion of exhaust heat into useful power would not just bring measurable advantages for improving fuel consumptions but also increase engine power density, further reducing CO_2 and other harmful exhaust emissions correspondingly.

Several direct and indirect energy recovery strategies have been developing by scientists and the automotive industry: the direct ones use gas enthalpy to drive an auxiliary turbine [2], while the indirect ones rely on the high gas temperature either to perform a direct conversion

of heat into electric power using thermoelectric generators [3] or applying innovative recovery approaches such as the realization of an additional expansion phase in a six-stroke engine cycle [4]. A more conventional methodology is the usage of exhaust gases as upper thermal source of a thermodynamic bottoming cycle such as Brayton, Stirling, Kalina and Rankine ones [5]. Among the indirect Waste Heat Recovery (WHR) methodologies, Rankine bottoming cycles that use an organic working fluid are characterized by high recovery potential as well as reduced investment costs [6]. However, although this idea of heat recovery was conceived in the 1970s, the industrial applicability of the technology still lacks of mature and reliable components, especially the pump and expander of the recovery system [7].

Recent literature reveals that an Organic Rankine Cycle (ORC) system equipped on an ICE might lead to a fuel economy up to 10-15% [8] and an overall efficiency increase up to 12% [9]. Besides, in reference studies [8, 10, 11] up to 20% of the waste heat from a heavy-duty diesel engine was recovered. As concerns light duty gasoline engines, an experimental analysis stated that at high engine powers, maximum efficiency of the ORC exhaust energy recovery system was up to 14%, and 3-8% under general vehicle operating conditions [12]. Researches on a heavy duty diesel engine using R141b as working fluid of the ORC system showed that engine efficiency increased by 3% and CO_2 emissions decreased by 150 tons/year. On the other hand, working fluids like R123 and water performed slightly worse [13].

Dual loop ORC systems to recover waste thermal energy both from engine exhaust gases and coolant were also developed: in a study on a gasoline engine as thermal source, it was concluded that engine efficiency increased up to 14-16% at peak power and up to 30-50% at lower loads [14]. For engine cooling water waste heat recovery, the use of regenerative ORC systems using R236fa and reheat regenerative ORC systems using R134a allowed to achieve an increase of ICE electrical efficiency up to 4.9% and a net efficiency of 6.6% [15].

Drawbacks due to vehicle weight increase and back-pressure effects along the exhaust gas path were recently outlined by the Authors to state the limits of a bottoming cycle energy recovery system in passenger cars and light-duty vehicles [16, 17].

In the current work, the development of an ORC-based energy recovery system for internal combustion engines is presented with respect to its design, measurement setup and experimentation. The novelty of the study relies on the usage of sliding vane machines for the expander and pump technologies. The recovery performances of sliding vane devices and ORC system were assessed through a test campaign at different engine operating regimes that led the recovery plant to work at design and off-design conditions.

2. Design Methodology

2.1. Exhaust gas mapping

The operating point of the engine, that can be expressed in terms of revolution speed (ω) and torque ($\widehat{T}$), highly affects mass flow rate and temperature of exhaust gases. Although the flexible nature of the internal combustion engine offers wide ranges of variation, in truck applications such as the ones for freight transportation, the vehicle mostly operates at cruise regime. For this reason, in order to design the energy recovery system, an experimental campaign at different stationary operating points was carried out on the IVECO F1C engine instrumented on the AVL APA 100 Transient dynamometer engine test bench complete with automation system based on Puma management software.

Exhaust gases were monitored downstream the particle trap to let the catalytic converter work in proper conditions. Main quantities of interest to design the recovery system were the gas mass flow rate and temperature. The first quantity resulted from the measurements of air and fuel mass flow rates while for the latter one a K-type thermocouple was used. Tests were carried out combining operating points at constant load (torque) with the ones at constant revolution speed. The region investigated is displayed in Figure 1 and covers those engine operating points

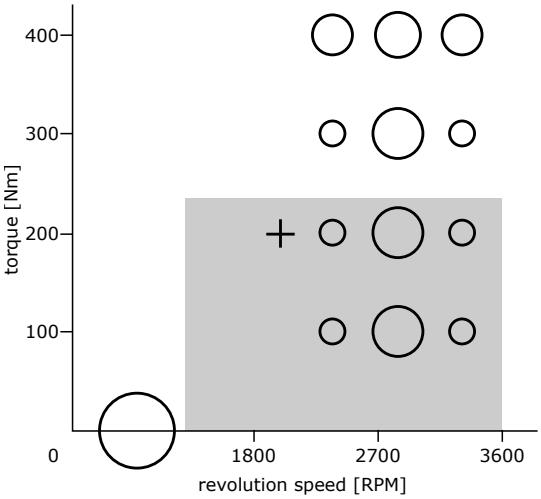

Figure 1. ESC and investigation area (grey region) - design point marked with a cross

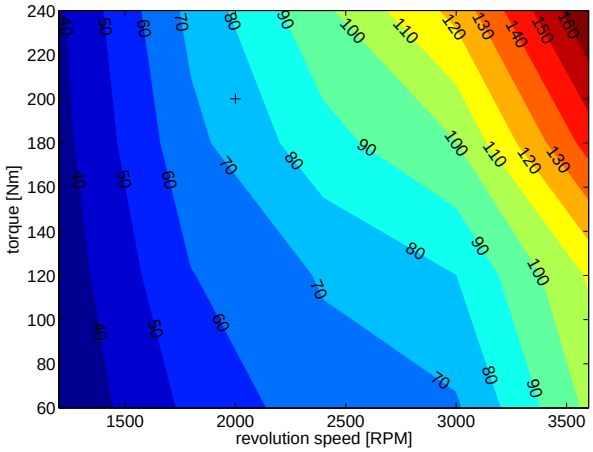

Figure 2. Exhaust gas mass flow rate [g/s]

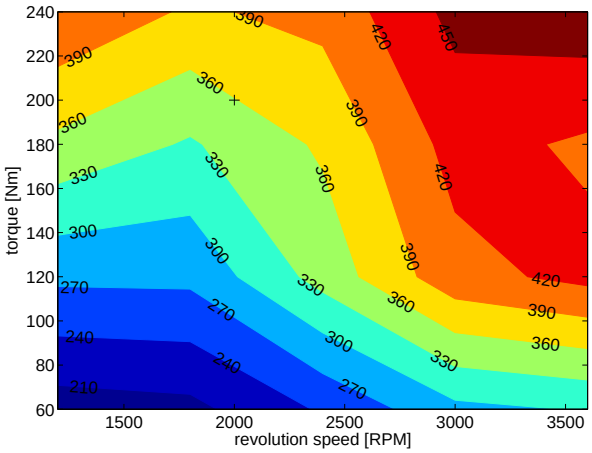

Figure 3. Gas temperature downstream the particle trap [°C]

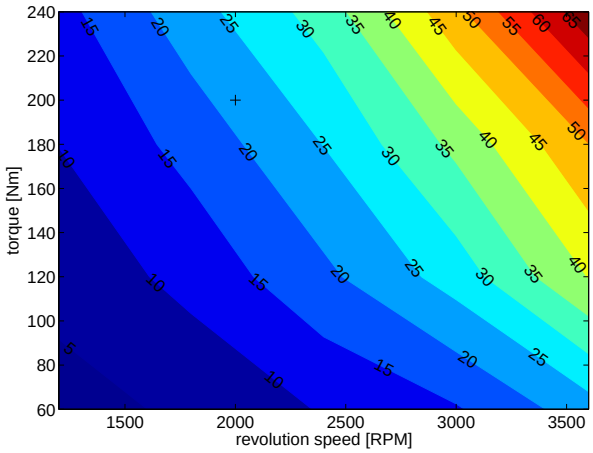

Figure 4. Available thermal power [kW] (discharge gas temperature 100 °C)

which commonly occur during driving conditions of freight transportation vehicles; it further embeds the bottom operating points of the ESC procedure (engine load at 25% and 50%).

As shown in Figures 2 and 3, there is a proportional dependence of exhaust gas mass flow rate and temperature with revolution speed and load. At high loads, gas temperature reached up 450 °C with a mass flow rate of 0.16 kg/s. With reference to an ideal heat transfer between gases and working fluid of the ORC-based recovery plant, assuming a specific heat at constant pressure for the gas of 1.1 $\mathrm{kJ\,kg^{-1}\,K^{-1}}$ and an outlet gas temperature of 100 °C, the thermal power that could be theoretically recovered is reported in Figure 4. The measurement uncertainty on the experimental characterization of the upper thermal source of the energy recovery plant did not exceed 1 % of the calculated value, as it resulted from the uncertainty propagation of the quantity measured.

Figure 3 shows higher gas enthalpy when load and revolution speed of the engine increase. Although from a pure thermodynamic viewpoint the design of the recovery system should be oriented to the maximum exergy of the upper thermal source, those regimes seldom occur

during the vehicle operation. Therefore, in order to maximize the energy recovery, the system was designed with reference to a usual operating point of the engine, namely 200 Nm at 2000 RPM.

2.2. Working fluid selection

The proper selection of the working fluid for the recovery plant is a fundamental step to achieve the best trade-off in terms of performance, costs and environmental requirements. In literature, several comprehensive studies provide suitable selection criteria [18]: fluids were mainly analyzed through a screening procedure based on thermodynamic performance [10, 19–21], preselected according to an idea of the operating map of the expansion device [22] or according to thermo-economic considerations [23]. Since the current research aimed at the development of machines for WHR, the thermodynamic approach was preferred.

Table 1. Input data for the thermodynamic analysis at design point

ICE at 200 Nm, 2000 RPM			Assumptions		
gas mass flow rate	$\dot{m}_g$	0.077 kg/s	cooling water inlet temperature	$T_{w,in}$	60 °C
gas inlet temperature	$T_{g,inl}$	356 °C	superheating	ΔT_{sh}	10 K
gas outlet temperature	$T_{g,outl}$	100 °C	subcooling	ΔT_{sc}	5 K

Among the assumptions and constrains listed in Table 1, the role of the superheating deserved a deeper analysis since the technological implications to enhance this parameter are rather challenging. A slight superheating always prevents liquid phase at the expander inlet. However, as demonstrated by the theoretical analyses reported in Figure 5, for a given available thermal power (like the one provided by the ICE at design conditions) cycle efficiency is not significantly affected. This fact, in disagreement with the steam power plant theory, is due to the shape of the saturation curve for wet and isentropic fluids. Indeed, the saturated vapor curve has a slope which always leads to a superheated state at the expansion end, even if expansion starts in saturated conditions. From that point on, since the slope of the upper and lower isobars is almost the same, an increase of superheating at the expansion inlet does not lead to benefits on the cycle efficiency.

The effects of superheating on the actual target performance parameters for waste heat recovery applications, i.e. the product between mass flow rate and net specific work, are further reported in non dimensional terms in the right chart of Figure 5. Unlike the other sensitivity analyses in which the cycle pressure ratio did not contribute to qualitatively modify the effects of superheating, the net power recovered is influenced both by the superheating and the cycle pressure ratio. Thermodynamic cycles with manometric pressure ratios (β_p) below 4 perform better if not superheated. On the other hand, maximum net power recovery would require superheating of the working fluid if the thermodynamic cycle operated at high pressure ratios. However, considering the theoretical approach of the analysis carried out and the minimal variation in percentage terms, it can be concluded that superheating does not contribute to enhance the recovery but it is highly advisable for technological reasons. In the current application, it was limited to 10 K.

On the other hand, a trade-off value of 5 K was assumed for the degree of subcooling at the condenser outlet in order to prevent cavitation phenomena at the pump without oversizing both condenser and evaporator because of a larger thermal power to reject or provide respectively (for a given maximum cycle temperature). Hence, the design choice of a large subcooling would have been twice disadvantageous in terms of weight and costs of the overall recovery system.

Main parameter investigated in the thermodynamic analysis was the cycle pressure ratio: since minimum pressure was constrained by the engine cooling system ($p_{min} > p_{sat}(T_{w,in})$),

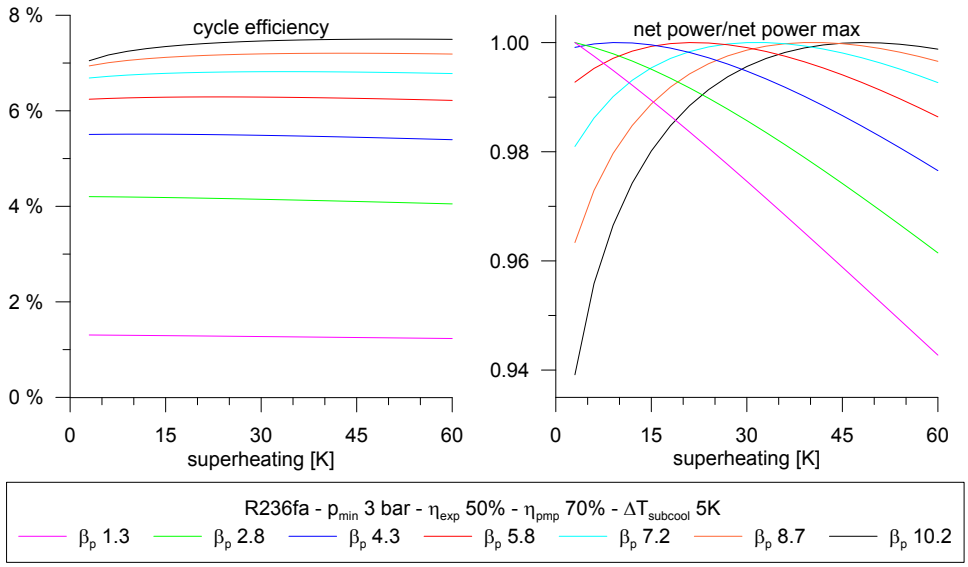

Figure 5. Effects of superheating on theoretical cycle performances

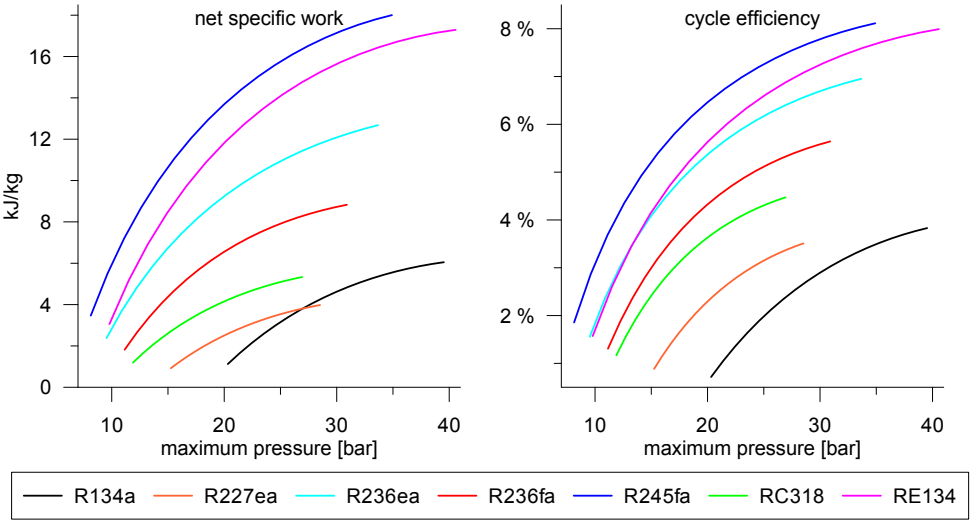

Figure 6. Working fluid selection

the maximum cycle pressure of the organic fluid was varied until 95 % of the critical threshold was reached. Results reported in Figure 6 show that R134a, R227ea and RC318 offer very low performance for the present application: they would require high flow rates and low pressure ratios to produce low net specific work and cycle efficiencies not exceeding 4 %. On the other hand, R245fa demonstrates the best theoretical performance as well as flexibility in the operating point (pressure ratio can vary from 1.5 to 5.5). At 30 bar the cycle efficiency would reach 7.7 % with a net specific work of 17.2 $\mathrm{kJ\,kg^{-1}}$ computed with a pump isentropic efficiency of 50 % and an expander isentropic efficiency of 70 %.

When cost variable was additionally taken into account as selection criterion, at this preliminary stage of the research the availability of R245fa became not affordable. Hence, the working fluid that was adopted for the development of the recovery system was R236fa (Hexafluoropropane with a $\mathrm{GWP_{100}}$ of 6300, an atmospheric lifetime of 209 years and a nil

Table 2. Theoretical design approaches (ICE at 200 Nm, 2000 RPM)

			vehicle-scale design	lab-scale design
fluid			R245fa	R236fa
maximum pressure	p_{max}	bar	30	15
minimum pressure	p_{min}	bar	6.2	3
working fluid mass flow rate	$\dot{m}_{WF}$	kg/s	0.098	0.109
expander volumetric flow rate	$\dot{V}_{WF,exp}$	L/min	31.38	64.38
pump volumetric flow rate	$\dot{V}_{WF,pmp}$	L/min	4.80	4.78
heat gain at the evaporator	$\dot{Q}_1$	kW	21.4	21.4
expander output power	$\dot{W}_{exp}$	kW	2.04	1.98
pump input power	$\dot{W}_{pmp}$	kW	0.38	0.19
cooling water mass flow rate	$\dot{m}_w$	kg/s	0.537	0.955
overall cycle efficiency	η_{ORC}	%	7.74	8.32

ODP).

2.3. Vehicle and lab-scale designs

In lab-scale tests, the availability of water at lower temperature ($T_{w,in} = 20$ °C), further allowed to decrease the pressure levels of the overall system at the same operating point of the internal combustion engine. Table 2 summarizes the operating parameters of the recovery system at design conditions with both the vehicle-oriented and lab-scale approaches: in both cases, cycle pressure ratio and mass flow rate are essentially the same while volumetric flow rate at the expander in vehicle-scale conditions is halved with respect to the laboratory ones. Therefore, the similarity study that led to the establishment of the design specifics for pump and expander of the recovery system led to the following conclusions:

- from a structural point of view, machines were designed with reference to the real operating conditions, whereas stresses are higher because of greater pressure values in the thermodynamic cycle;
- since inlet conditions at the pump led to the same volumetric flow rate, operating conditions in lab-scale tests actually simulate the vehicle application;
- at this stage of development, the reference specifics for the expander design were the laboratory ones. To restore the volumetric flow rate at design point in vehicle operating conditions, the expander should work at 50 % of the revolution speed. If the machine was coupled with a DC generator (or an AC generator with AC/DC converter) to store the energy recovered in the batteries, this requirement would be effortlessly achievable.

3. Experimental Setup

The power unit displayed in Figure 7 is able to recover heat from the exhaust gases of the IVECO F1C engine and converts it into electrical energy. The working fluid (a mixture of R236fa and 5% of POE oil) accomplishes a series of thermodynamic transformations according to a slightly superheated Rankine cycle. The heat recovery takes place downstream the particle trap of the engine and allows pre-heating, vaporization and superheating of the working fluid that further expands in the sliding vane expander. The mechanical energy recovered is eventually converted into electric energy through an asynchronous generator. After the expansion process, the organic fluid is de-superheated and condensed using water as lower thermal source. The recovery system

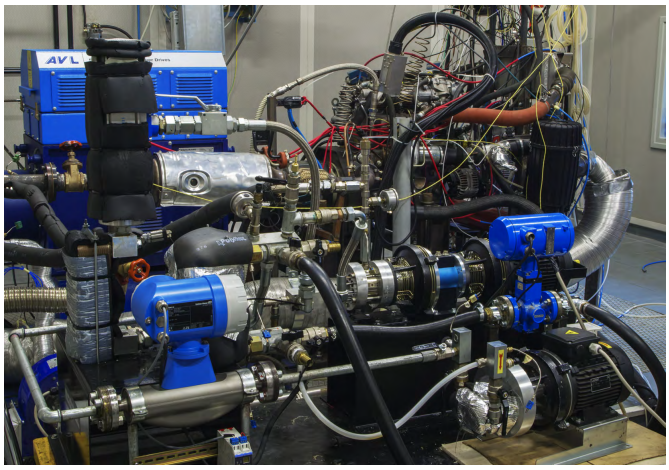

Figure 7. Engine and ORC system test benches

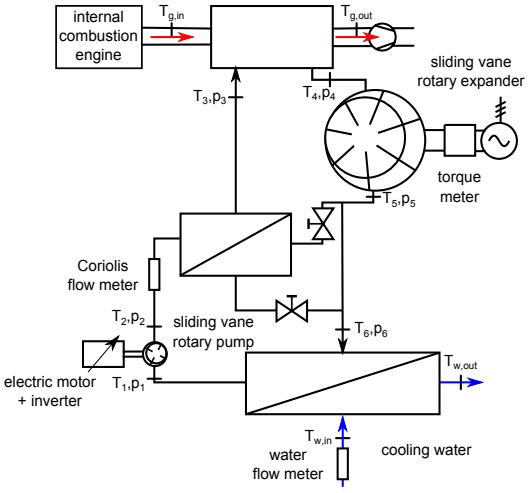

Figure 8. Plant layout and instrumentation

layout can also take into account regeneration. At the condenser outlet, the working fluid reaches a sub-cooled state to be properly pressurized by the sliding vane rotary pump. An inverter on the electric motor of the pump allowed to vary the mass flow rate circulating in the plant while the expander rotated at revolution speeds slightly grater than 1500 RPM, constrained by the electric grid frequency.

Pressure and temperature transducers were installed across all the plant components, as reported in Figure 8. Due to their limited operating range, gas temperatures across the hot side of the evaporator were monitored using K-type thermocouples instead of T-type ones used elsewhere. The sliding vane expander performances were assessed through a direct measurement of mechanical power as product of torque and revolution speed measured by a torque meter. A Coriolis mass flow meter with a HART loop converter was installed downstream the pump and allowed a direct measurement of the working fluid mass flow rate as well as its temperature and density at the same location.

Pressure and temperature data acquired during the tests were linked to the Coolprop LabVIEW library to retrieve all the thermophysical properties of the working fluid in the measuring points. In this way, the real-time entropy diagram was graphed to provide immediate information on the recovery system behavior. At the same time, energy balances were implemented in a graphical interface.

4. Results and Discussion

The test campaign was performed in stationary conditions for the internal combustion engine and the recovery power unit in order to investigate the behavior of both systems and their reciprocal influence. The reference test conditions were chosen according to the operating points of the European Stationary Cycle (ESC), a 13-mode steady state procedure used for emission measurement from heavy-duty diesel engines (Directive 1999/96/EC). However, in order to assess an effective heat recovery from the engine, the idle operating point shown in Figure 1 was not considered. In particular, since operating regimes between engine loads at 25% and 50% are the typical driving conditions of freight transportation vehicles, thus the ones in which the energy recovery would effectively impact on the overall fuel savings in absolute terms, results are presented for six test cases and summarized in Table 3.

Figure 9 details the test case closest to the design point (200 Nm, 2175 RPM) with absolute

Table 3. Test matrix

$\widehat{T}_{ICE}$	Nm	100	200	100	200	91	182
ω_{ICE}	RPM	2175	2175	2750	2750	3325	3325
$\dot{m}_g$	kg/s	0.063	0.080	0.073	0.100	0.077	0.114
$T_{g,inl}$	°C	304.2	350.2	346.4	364.2	422.9	431.2
$T_{g,outl}$	°C	71.4	90.8	85.5	106.4	101.5	137.0
$\dot{m}_{WF}$	kg/s	0.101	0.139	0.127	0.179	0.167	0.208
p_{max}	bar	9.8	13.7	12.5	17.4	16.9	21.9
β_{exp}	-	2.5	2.8	2.9	3.2	3.3	3.4
T_{max}	°C	72.7	89.0	84.8	101.0	100.1	119.5
T_{min}	°C	29.0	36.8	33.5	41.5	40.1	48.4
$\widehat{T}_{exp}$	Nm	4.25	6.68	6.27	8.66	8.24	11.24
ω_{exp}	RPM	1535	1569	1553	1573	1572	1606

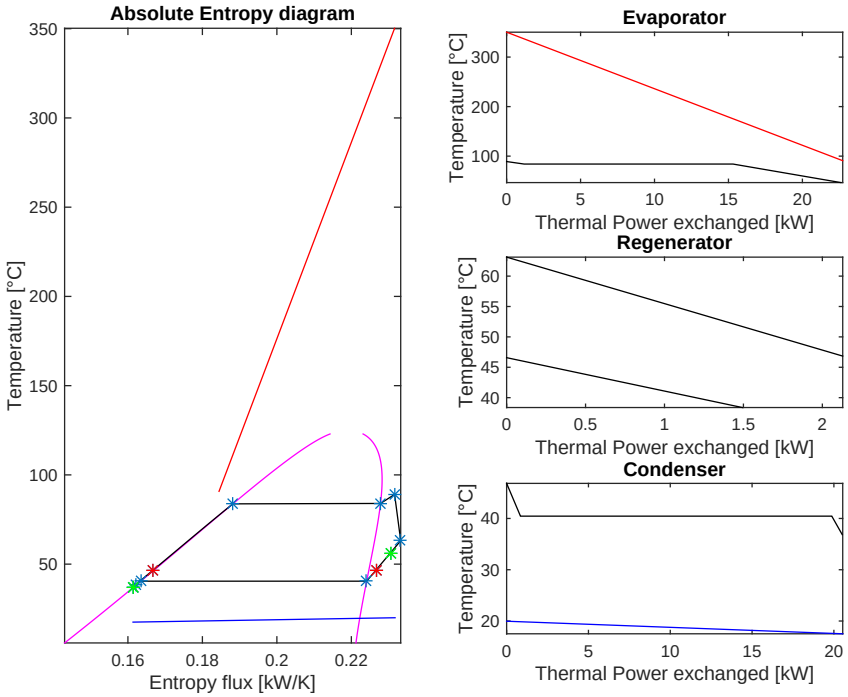

Figure 9. Thermodynamic summary - 200 Nm, 2175 RPM

entropy diagram and heat transfer curves at evaporator, condenser and recuperator. Since the first two devices were carefully insulated, the efficiency of the heat transfers from the exhaust gases to the working fluid and from the working fluid to the cooling water reveals almost unitary. Conversely, in the recuperator, thermal losses to the environment reduced the amount of regeneration. In particular, the share of regenerated power over the total gain at the regenerator and the evaporator was limited between 5% and 10%. In all the experiments, the pinch point at the evaporator occurred between working fluid inlet and gas outlet. Furthermore, the significant gap between red and black curves reveals high irreversibilities in the heat transfer.

Figures 10 and 11 provide a summary of the recovery performance of the ORC system achieved in the 6 ESC points. Energy recovery increases at higher loads and engine revolution speeds

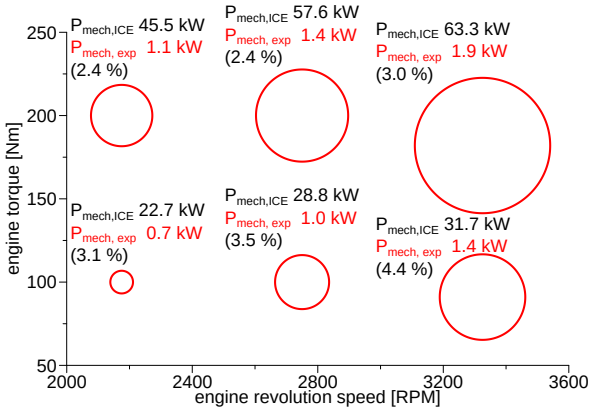

Figure 10. Summary of the energy recovery performances

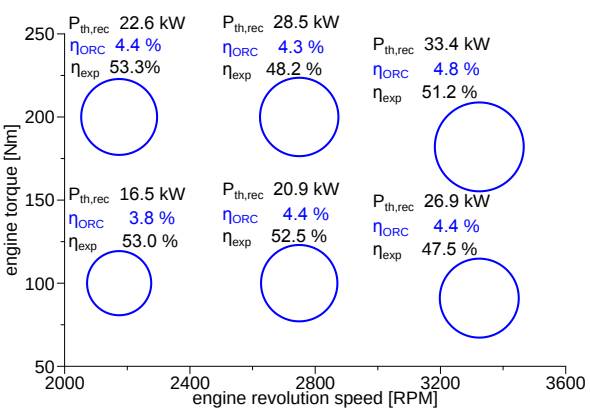

Figure 11. Summary of the energy recovery efficiencies

due to greater exhaust gas mass flow rates and temperatures. At 3225 RPM and 182 Nm, the sliding vane expander was able to provide up to 1.9 kW in mechanical form (3% of the engine power). Additionally, overall cycle efficiency reached 4.8%. Although the availability of the thermal waste decreased at low regimes, the recovery system was able to perform efficiently also at off-design conditions. At 3225 and 91 RPM, mechanical power at the expander shaft reached 4.4% of the engine shaft power. In all the experiments, overall efficiency of the power unit was always around 4%.

As concerns the global expander efficiency, computed as ratio of the mechanical power over the isentropic power, best performances occurred in the test case closest to the design point (η_{exp} 53.3%). At off-design conditions with higher heat gain, mechanical power recovered increased due to a higher working fluid mass flow rate and cycle pressure ratio. However, the large superheating that characterized these operating points worsened the expander efficiency because of greater discharge pressures at the condenser.

A more extensive investigation of the fluid behavior within the machine might be provided retrieving the expander indicator (pressure-volume) diagram from high frequency pressure data. This activity was previously carried out by the Authors in [24] with the methodology developed for sliding vane compressors [25] and it will be performed in the near future on this application using piezoresistive pressure transducers rather than piezoelectric ones in order to minimize the measurement uncertainty due to the reconstruction procedure of the pressure-volume diagram [26, 27].

5. Conclusions

Bottoming organic Rankine cycles for the energy recovery from exhaust gases of internal combustion engines recently gained the attention of scientific community and automotive industry thanks to their remarkable theoretical performances and economic feasibility. In this context, the current research work dealt with the design, development and testing of an ORC-based recovery power unit. The novelty of the study was the usage of the sliding vane technology for pump and expander of the recovery system in order to face the lack of mature, efficient and reliable devices for waste heat recovery in automotive applications.

Power unit design was carried out after an experimental campaign on an IVECO F1C engine that assessed the available thermal power at the engine exhaust. Two design configurations were compared to reproduce vehicle operating conditions in laboratory tests. The experimental test bench of the ORC recovery system equipped with sliding vane machines was characterized by

a high-accuracy measurement chain and a data acquisition routine that also provided the real-time entropy diagram as monitoring tool during the experiments. Recovery system performances were experimentally assessed through a steady test campaign where the ORC power unit was coupled with the internal combustion engine. Mechanical power recovery reached up to 1.9 kW which corresponded to 3% of the engine mechanical power at that given operating conditions. This share increased at low engine loads and high revolution speeds. The overall cycle efficiency ranged between 3.8% and 4.8%, while the overall expander efficiency values were between 47.5% and 53.3%.

Improvements on the overall cycle efficiency are expected thanks to an upgraded plant layout and thermal insulation of the components. Greater isentropic and volumetric efficiencies of the sliding vane expander are going to be achieved optimizing intake and exhaust processes. These activities will be supported by the analysis of the expander indicator diagram using high frequency pressure sensors to investigate the fluid pressure evolution within the machine.

Acknowledgement

Ing. Enea Mattei S.p.A., in the persons of Dr. Giulio Contaldi and Dr. Stefano Murgia, is gratefully acknowledged for the technical support provided throughout the development of sliding vane expander and pump prototypes.

References

[1] IEA 2014 *Key world energy statistics* (International Energy Agency)
[2] Weerasinghe W, Stobart R and Hounsham S 2010 *Applied Thermal Engineering* **30** 2253 – 2256
[3] Riffat S and Ma X 2003 *Applied Thermal Engineering* **23** 913 – 935
[4] Conklin J C and Szybist J P 2010 *Energy* **35** 1658 – 1664
[5] Sprouse C and Depcik C 2013 *Applied Thermal Engineering* **51** 711 – 722
[6] Saidur R, Rezaei M, Muzammil W, Hassan M, Paria S and Hasanuzzaman M 2012 *Renewable and Sustainable Energy Reviews* **16** 5649 – 5659
[7] Lopes J, Douglas R, McCullough G, O'Shaughnessy R and et al 2012 *SAE Technical Paper* **2012-01-1942**
[8] Teng H, Klaver J, Park T, Hunter G L and van der Velde B 2011 *SAE Technical Paper* **2011-01-0311**
[9] Vaja I and Gambarotta A 2010 *Energy* **35** 1084 – 1093
[10] Teng H, Regner G and Cowland C 2007 *SAE Technical Paper* **2007-01-0543**
[11] Teng H and Regner G 2009 *SAE Technical Paper* **2009-01-2913**
[12] Wang T, Zhang Y, Zhang J, Shu G and Peng Z 2013 *Applied Thermal Engineering* **53** 414 – 419
[13] Wang T, Zhang Y, Zhang J, Peng Z and Shu G 2014 *Energy Conversion and Management* **84** 97 – 107
[14] Arias D A, Shedd T A and Jester R K 2006 *SAE Technical Paper* **2006-01-1605**
[15] Peris B, Navarro-Esbr J and Mols F 2013 *Applied Thermal Engineering* **61** 364 – 371
[16] Di Battista D, Mauriello M and Cipollone R 2015 *Applied Energy* **152** 109 – 120
[17] Di Battista D, Mauriello M and Cipollone R 2015 *SAE Technical Paper* **2015-01-1608**
[18] Bao J and Zhao L 2013 *Renewable and Sustainable Energy Reviews* **24** 325 – 342
[19] Wang Z, Zhou N, Guo J and Wang X 2012 *Energy* **40** 107 – 115
[20] Tian H, Shu G, Wei H, Liang X and Liu L 2012 *Energy* **47** 125 – 136
[21] Liu B T, Chien K H and Wang C C 2004 *Energy* **29** 1207 – 1217
[22] Quoilin S, Declaye S, Legros A, Guillaume L and Lemort V 2012 *Working fluid selection and operating maps for Organic Rankine Cycle expansion machines*
[23] Quoilin S, Declaye S, Tchanche B F and Lemort V 2011 *Applied Thermal Engineering* **31** 2885 – 2893
[24] Cipollone R, Bianchi G, Di Battista D, Contaldi G and Murgia S 2014 *Energy Procedia* **45** 121 – 130
[25] Bianchi G and Cipollone R 2015 *Applied Energy* **142** 95 – 107
[26] Bianchi G and Cipollone R 2015 *Applied Thermal Engineering* **84** 276 – 285
[27] Bianchi G, Cipollone R, Murgia S and Contaldi G 2015 *International Journal of Refrigeration* **52** 11 – 20